COMPDYN 2013
4th ECCOMAS Thematic Conference on
Computational Methods in Structural Dynamics and Earthquake Engineering
M. Papadrakakis, V. Papadopoulos, V. Plevris (eds.)
Kos Island, Greece, 12–14 June 2013

CABLE-STAYED BRIDGES SUBJECTED TO NEAR-FAULT VERTICAL MOTION

M. Kuleli[1] **and A. S. Elnashai**[1]

[1] Department of Civil and Environmental Engineering, University of Illinois at Urbana-Champaign, USA
e-mail: {kuleli2, aelnash}@illinois.edu

Keywords: Vertical Ground Motion, Near-Fault Effects, Cable-Stayed Bridge.

Abstract. *The existence of a horizontal large velocity pulse that contains a substantial proportion of the seismic energy, often referred to as a 'fling', tends to increase seismic demand on medium-to-long period structures. Vertical ground motion is most intense and damaging in near-fault region, which openings the possibility that vertical motion may also include strong velocity pulses. An investigation of possible 'fling' features in vertical ground motion and their effects on cable-stayed bridge structures is presented in this paper. It is endeavored to identify and explain the reasons for strong velocity pulses in vertical ground motion. A set of earthquake records from recent large thrust events, which provided abundant near-fault vertical ground motion records, was selected and analyzed to identify large velocity pulses. Comparison is made with a set of normal acceleration records. Detailed numerical models of a class of cable-stayed bridges were developed, based on an existing bridge structure. The strong-motion ensemble is used for dynamic geometrically-nonlinear response history analysis of the cable-stayed bridges. Global and local response parameters were monitored and compared. The results indicate that pulse-like vertical ground motion increases moment and rotation demands along the bridge deck and should therefore be considered in seismic design and assessment.*

1 INTRODUCTION

The vertical component of earthquake ground motion has only recently received considerable investigative attention. In contrast, both near- and far-fault horizontal seismic excitations have been extensively studied and considered in the design process. One of the most important features of near-fault ground motions is the presence of strong velocity pulses. Strong velocity pulses cause most of the seismic energy from the rupture zone to arrive during a short period of time. Investigations on pulse-like horizontal ground motion in the last few decades have highlighted their distinct seismic response amplification characteristics. It was shown that pulse-like ground motion tends to amplify the seismic demand in the long period range of the acceleration response spectrum [1]. Furthermore, many studies investigated the seismic response characteristics of building structures subjected to pulse-like horizontal ground motion. It was indicated that strong velocity pulses tend to result in higher inelastic demands on buildings that have long fundamental periods [2, 3] and the structures in the intermediate-to-long period range are more susceptible to directivity pulses in horizontal ground motion [4, 5]. Moreover, it was suggested that the pulse-like ground motion forces the structure to dissipate the seismic energy input in a short period of time with a few inelastic cycles and hence increase the ductility demand [6, 7]. Moreover, recent studies of the engineering seismology community on the dynamics of faults have revealed that vertical ground motion may also contain strong velocity pulses. However, the effects of pulse-like vertical ground motion have not been studied by the structural engineering community before.

Recently a limited number of studies suggested that the vertical ground motion may increase not only the axial force demand on columns and piers but also the bending moment demand on bridge girders. The effects of vertical ground motion on precast segmental bridge girders were investigated with 2D models which were based on the Otay River Bridge and the San Francisco-Oakland Bay Bridge [8]. A suite of ten near-fault earthquake records were employed to perform non-linear time history analyses. It was concluded that segment joint rotations increased at least 400% and 90% for negative and positive bending moment, respectively as a result of the vertical ground motion. Furthermore, a parametric study on two short span reinforced concrete bridges considering various span lengths and pier heights was conducted to investigate the effects of vertical ground motion [9]. Although the focus of the study was on the pier response, it was consistently observed that the bending moment demand on the girders at the face of the bent cap was amplified. It was concluded that the contribution of the vertical ground motion to the moment demand was up to 155% and scaled with the V/H ratio. Six different configurations of ordinary standard highway bridges and overcrossings were utilized to investigate the effects of vertical ground motion on the response of bridge decks [10]. A data set of 56 records was formed based on horizontal peak accelerations (> 0.5g). The results of the nonlinear time history analysis were presented relative to the dead load demands to provide a comparison with the Seismic Design Criteria 2006 (SDC) guidelines. It was concluded that the negative bending moment demands at the mid-span (center of the main span) and positive bending moment demands at the face of the bent cap were significantly increased when the vertical ground motion was included in the analysis.

In this study, it is endeavored to identify and explain the reasons for strong velocity pulses in vertical ground motion. Previous studies on dynamics of faults are summarized. A ground motion selection procedure is described. Furthermore, the effects of pulse-like vertical ground motion on a class of cable-stayed bridges were investigated through detailed numerical models.

2 NEAR-FAULT EFFECTS IN VERTICAL GROUND MOTION

Directivity, fling step and existence of asperities are the reasons for strong velocity pulses in ground motion. Near-fault horizontal ground motion have been extensively studied and considered in the design process. Especially, directivity effects of fault-normal component resulting from strike-slip events have been investigated extensively in the last two decades. However, recent studies on fault dynamics, supported with increasing numbers of near-fault records (especially after the 1999 earthquakes), suggest that near-fault effects in vertical ground motion may have been underestimated.

2.1 Strong velocity pulse

Forward directivity is caused by constructive interference of shear waves when rupture propagates toward a site at a velocity close to the shear-wave velocity. Furthermore, fling step is the tectonic deformation associated with the permanent static offset of the ground due to surface rupture. In strike-slip events (Figure 1a), directivity and fling step effects are polarized on two components; strike-normal and strike-parallel, respectively. Therefore, directivity and fling step effects are usually considered uncoupled. Forward directivity and fling step effects can also occur on dip-slip faults [11]. For example, Figure 1b and 2 illustrate the orientation of the slip vector and rupture propagation in a thrust fault mechanism, respectively. The plane perpendicular to fault plane represents the neutral directivity orientation. The slip vector and rupture propagation both directed toward up dip. Shear waves travelling toward the site constructively interfere with each other in both vertical (Figure 2) and horizontal (strike-normal) directions. Therefore, the site located above the neutral plane is forward directivity site. Furthermore, fling step effects are also directed up-dip aligned with the slip vector. Thus, strong velocity pulses due to directivity and fling step effects are coupled on the vertical component and the horizontal component (strike-normal) of ground motions [12].

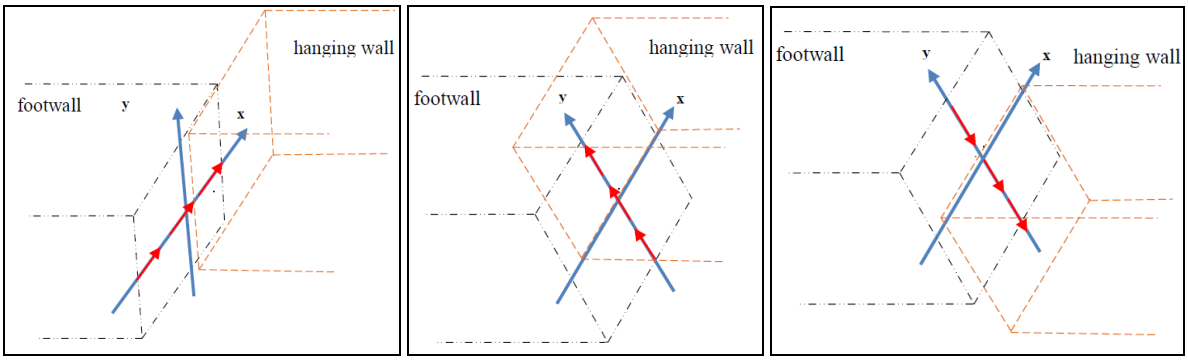

(a) Strike-slip fault (b) Thrust fault (c) Normal fault

Figure 1: Rupture and slip directions of symmetric and asymmetric faults

The third contributor to strong velocity pulses in vertical ground motion is the hanging wall effect [13]. As the rupture propagates towards up-dip a gap is formed between the hanging wall and footwall of the fault. The seismic energy is trapped between two opaque surfaces; the gap on the fault plane and the free field. Greater particle motion was observed on the hanging wall of thrust faults due to continuous reflection of seismic waves between the two surfaces during the rupture propagation [13]. This physical phenomenon has been also supported by many analytical [14, 15, 16] and experimental studies [17, 18, 19, 20] conducted to understand the ground motion characteristics resulted from asymmetric fault events.

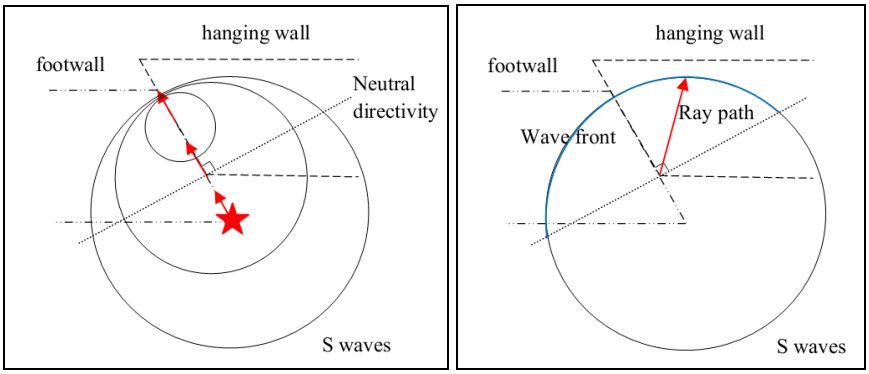

Figure 2: Directivity and fling step orientation in thrust fault mechanism

Furthermore, the directivity model which has been used so far is a one dimensional model which assumes a unidirectional rupture [11]. In strike-slip fault events, the rupture is assumed to be oriented only in the strike direction and the heterogeneities in depth are ignored. Similarly, in the case of dip-slip faults the rupture is assumed to propagate only in the dip direction hence is independent of heterogeneities along the strike direction. The assumption of unidirectional rupture led to two results. First, the widely accepted velocity pulse definition considers only the largest velocity cycle. Second, the directivity effects in dip-slip events are assumed to be concentrated only on the region located directly above the hypocenter.

However, rupture heterogeneity may arise from many reasons such as; existence of asperities or irregularities in the geometry of the fault (i.e. asymmetric faults). Large magnitude earthquakes are especially likely to be far from homogeneous [21]. When rupture heterogeneity is considered, multiple velocity cycles should be taken into account. Recently, a strong relationship between directivity pulses and slip heterogeneity was observed and a new ground motion selection procedure, which considers multiple velocity cycles, was suggested [22]. This selection procedure is further discussed in the following section.

Moreover, vertical ground motion is often assumed to be more of a manifestation of P-waves. However, it has been proven that when the crustal heterogeneity and source finiteness in vertical extent is considered, SV waves also significantly contribute to vertical ground motion in near-fault sites due to the refraction on certain horizontal boundaries [23]. The distance where SV waves are dominant may be extended to 10~20km [24]. Thus, strong velocity pulses in vertical ground motion can be observed not only in the region concentrated up dip from the hypocenter but also in the near-fault region where SV wave contribution is not negligible.

Near-fault effects on vertical component may also be observed in oblique, normal and even in strike-slip fault events depending on the rupture propagation and slip directions. However, strong velocity pulses in vertical ground motion are most prominent in thrust fault mechanism due to coupling of directivity, fling and hanging wall effects as explained above. Thus, in this study only recent thrust events which provided abundant near-fault ground motion records are considered.

2.2 Characteristics of pulse-like vertical ground motion

91 records from four recent large thrust events are selected to investigate the characteristics of pulse-like vertical ground motion. These events are as follows: 1994 Northridge (US), 1999 Chi-Chi (Taiwan), 2010 Darfield (New Zealand) and 2011 Christchurch (New Zealand). The selection of the records is based on the following criteria: 1) peak vertical acceleration (PVA) $\geq$ 0.1g, 2) peak vertical velocity (PVV) $\geq$ 10 cm/s, 3) Mw $\geq$ 6.0, epicentral distance < 25 km or closest distance < 20 km (when available).

Two procedures were proposed to identify pulse-like horizontal ground motion. The first procedure is described as follows [25]: The largest velocity pulse which starts and ends at zero crossing times or where the velocity is equal to 10% of the peak ground velocity [26] is extracted from the original record by using a wavelet-based signal processing analysis. The remaining record is designated as the residual record. The classification of the signals is defined by two parameters. The first parameter is the peak ground velocity (PGV) ratio which is defined as the PGV of the residual record divided by the PGV of the original record. The second parameter is the energy ratio which is the ratio of the energy of the residual record to the energy of the original record. Moreover, pulse period (single cycle) is determined using the period corresponding to the maximum Fourier amplitude of a wavelet. Recently, a new ground motion selection procedure, which considers multiple velocity cycles, was suggested [22]. This procedure uses a velocity pulse definition based on a specific level of threshold energy. By inspection of the selected 308 horizontal ground motion records, this threshold energy is designated as 35% of the total energy of the original record which is carried by certain number of cycles. The maximum number of cycles is specified as three. Furthermore, a new pulse period definition called, Tp^{eff}, effective pulse period was also proposed. Tp^{eff} is designated as the time width of the total velocity cycles which corresponds to the specified threshold energy. It is also concluded that the effective pulse period is more related to the magnitude of the event than the period of a single cycle.

In this study, the ground motion selection procedure proposed by [22] is modified to fit natural trend of the selected vertical ground motion records. First, velocity time histories of each record are inspected manually and the data set is grouped in two categories. The first group of ground motions is those which contain "coherent" pulses (Figure 3a) and the second are those which contain "incoherent" pulses (Figure 3b). Here a coherent pulse refers to a wave signal that consistently keeps the increasing or decreasing trend in local and global levels. On the other hand, an incoherent pulse refers to a signal that is less coherent at the local level (sometimes including several zero crossings) yet keeps its increasing/decreasing global trend through the velocity time history. For example, the spikes in signal at the local level can be seen in Figure 3b. On the other hand, the global increasing/decreasing trends of the signal at the global level are also shown by the black arrows in Figure 3b. Although the energy concentration is continuous in the case of incoherent pulses, it results in response amplification in a shorter period range when it is compared to their coherent counterparts. Because the shorter the predominant period of the ground motion, the smaller is the period range at which the response amplification occurs.

It has been consistently observed that the ground motions which have up to four successive full velocity cycles tend to exhibit pulse-like characteristics. For each record the cycle with highest amplitude (PGV) is obtained using zero crossing time definition. Then, the successive (or preceding) velocity pulse which has minimum amplitude of about 50% of the amplitude of the preceding/following half cycle is determined. The minimum considered amplitude of a half cycle is 10 cm/s which are of engineering interest. For each record, the wave trains which contain up to four full cycles are extracted from the original record. It is important to note that, for records which have $10 < PGV < 20$ cm/s, the half cycles with 10cm/s or less amplitude are also included in the wave train to be in accordance with the selection criteria of half cycle which has a minimum amplitude of about 50% of the amplitude of the preceding/following half cycle. After extraction of the wave train, the ratio of the energy of the residual record to the energy of the original record is calculated. The energy of each record is calculated as the integration of the squared velocity time history. It has been consistently observed that records which contain strong velocity cycles (up to four cycles) and have an "energy ratio" smaller than a certain threshold level tend to exhibit "pulse-like" characteristics which result in ampli-

fication of response in the medium-to-long period range. The limits of the energy ratio are presented in Table 1. Here it is important to note that the energy ratio limits for classification of the incoherent records are smaller than their coherent counterparts due to their different response amplification. For instance, when two wave trains of the same PGV, number of cycles and their amplitudes and same total period are considered, the coherent record provides higher seismic energy than the incoherent record and hence results in higher response amplification. As incoherency increases, ground motions tend to exhibit ordinary characteristics where response amplification is most effective in very short period range (< 0.5sec).

	Energy Ratio		
	min	max	Class
Coherent	0.0	0.4	Pulse
	0.4	0.6	Ambiguous
	0.6	1.0	Ordinary
Incoherent	0.0	0.2	Pulse
	0.2	0.4	Ambiguous
	0.4	1.0	Ordinary

Table 1: Energy ratio intervals for ground motions

Figure 3 represents original and residual velocity time history records of a coherent pulse-like, an incoherent pulse-like and an ordinary vertical ground motion, and their acceleration response spectra. From Figure 3 it is evident that ordinary vertical ground motions are most effective in the small period range where the pulse-like ones tend amplify the response in medium-to-long period range of response.

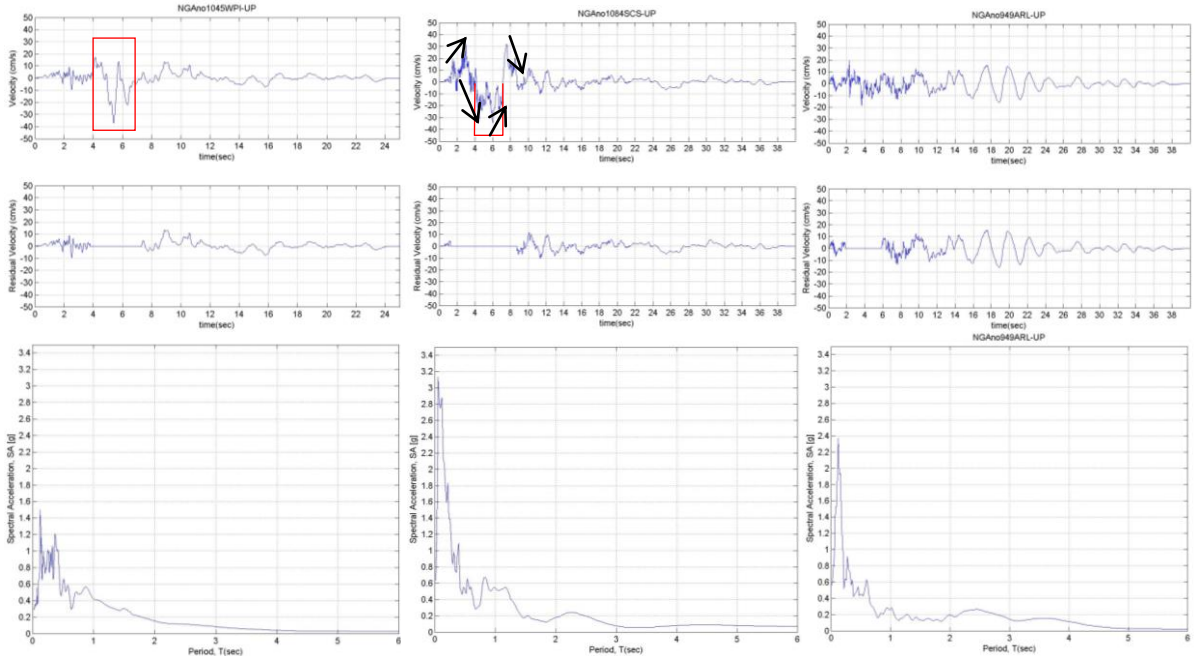

(a) (b) (c)

Figure 3: Original and residual velocity record of (a) Newhall – W Pico Canyon Road (coherent pulse) (b) Sylmar – Converter (incoherent pulse) (c) Arleta-Nordoff Fire Stations (ordinary) from Northridge, 1994

Furthermore, Figure 4 compares the frequency content of representatives of a pulse-like and an ordinary vertical ground motion. It can be seen that ground motion records classified as "pulse-like" tend to have smaller frequency contents when compared to ordinary counterparts. Thus, it can be concluded that the presence of strong velocity pulses in vertical ground motion tend to amplify the response not only in the short period range but also in the medium-to-long period range of vertically vibrating structures.

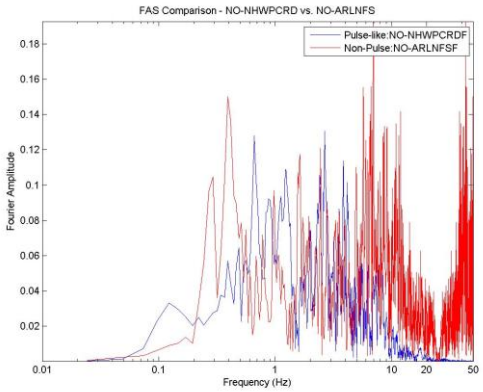

Figure 4: Frequency content comparison for Newhall – W Pico Canyon Road (coherent pulse) Arleta-Nordoff Fire Stations (ordinary) from Northridge, 1994 Earthquake

In summary, 44 of the 91 ground motions in the data set were classified as pulse-like, 29 of them were classified as ambiguous and 18 of them were classified as ordinary vertical ground motions. Here it is important to note that an ambiguous class may contain both pulse-like and ordinary ground motions. Further study is needed for more elaborate classification of this class.

3 ANALYTICAL INVESTIGATION

This study focuses on the investigation of the effects of the pulse-like vertical ground motions on a class of medium-to-long-span bridge girders. Cable-stayed bridges are sensitive to three dimensional earthquake excitations due to the strong coupling between their modes of vibration in the three orthogonal directions unlike such as suspension bridges where modes of vibration can be categorized as bending, torsional and sway [27]. Thus, a class of cable-stayed bridge configurations was chosen to represent medium-to-long span length which allows seismic response assessment over a large range of periods.

3.1 Structural modeling and dynamic characteristics of the selected bridges

The general and tower configurations of a class of cable-stayed bridges are depicted in Figures 5 and 6 [27]. The main span lengths are 1120 and 2200 ft. for Bridge I and Bridge II, respectively.

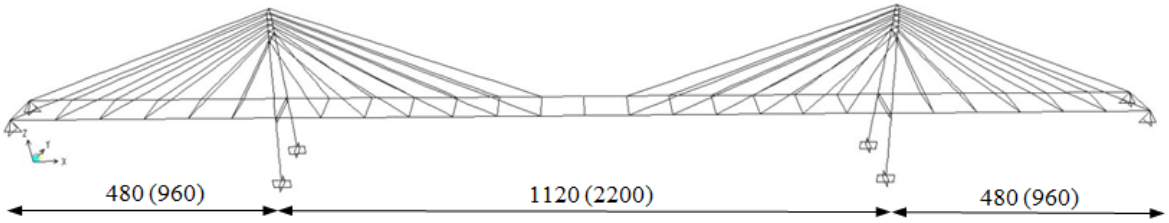

Figure 5: Cable and deck configuration of Bridge I (Bridge II), units: ft.

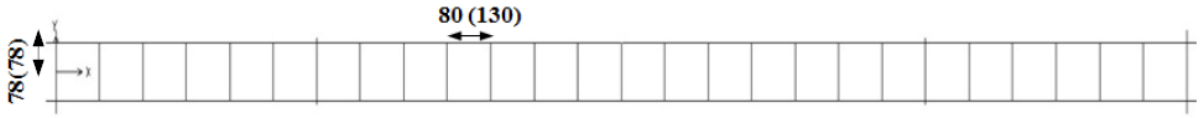

Figure 5 (cont'd): Cable and deck configuration of Bridge I (Bridge II), units: ft.

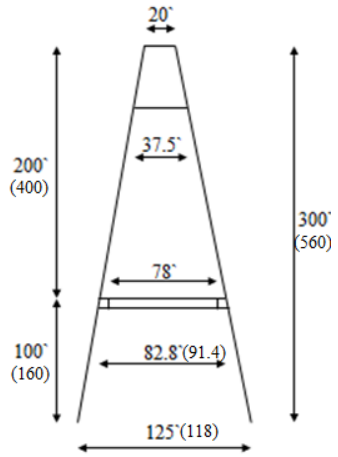

Figure 6: Tower configuration of Bridge I (Bridge II), units: ft.

Cable-stayed bridges are sensitive to three dimensional excitations due to the strong coupling between modes of vibrations. Thus, detailed three dimensional models are developed to account for torsional effects and torsional modes of vibration. The structural properties of the elements in these two bridges were based on several existing bridges in the eastern region of the United States and further details of the section and material properties can be found in [27]. Each cable is represented by a single bar element with equivalent tangent (or instantaneous) modulus approach. Reinforced concrete pylons, pylon struts and steel girders and cross beams are modeled with elastic beam elements. The decks are simply supported at both ends of the girder and connected to the pylons and pylon struts with the elastic links as depicted in Figures 5 and 6.

Static nonlinear analyses which include P-Delta effects are conducted for dead loads to obtain the tangent stiffness matrix of the structures. The dead load tangent stiffness is employed as the initial stiffness for all other analysis cases, namely live load, modal analysis and nonlinear time history analysis. Eigen value analyses are performed to obtain dynamic behavior characteristics with utilization of the tangent stiffness matrix of the dead load deformed state. 200 modes are employed to obtain 95% or higher mass participation in longitudinal, transverse and vertical directions. The first modes of cable-stayed bridges are usually deck modes, followed by coupled cable and deck modes and coupled tower and deck modes [28]. Thus, deck modes are coupled with all other modes through almost all 200 modes of vibrations and cover a period range from 3.25s to 0.027s for Bridge I and from 5.13s to 0.05s for Bridge II. Accumulated mass participation ratios in the vertical direction over the periods of vibration modes for both Bridges I and II are depicted in Figure 8. Hence deck modes of Bridge I and II cover a large period range in vertical direction, the effects of pulse-like and ordinary vertical ground motions can be investigated.

3.2 Selection of strong ground motion

4 raw ground motion records from "coherent pulse-like", 3 records from "incoherent pulse-like" and 4 records from "ordinary" classes were selected as shown in the Table 2. The peak

acceleration ratios of the vertical to horizontal component (V/H), identified pulse period of wave trains (Tp^{wt}) and the energy ratios of the residual record to the original record are also listed in Table 2. Time lag effects between the vertical and horizontal ground motion peaks were not taken into account.

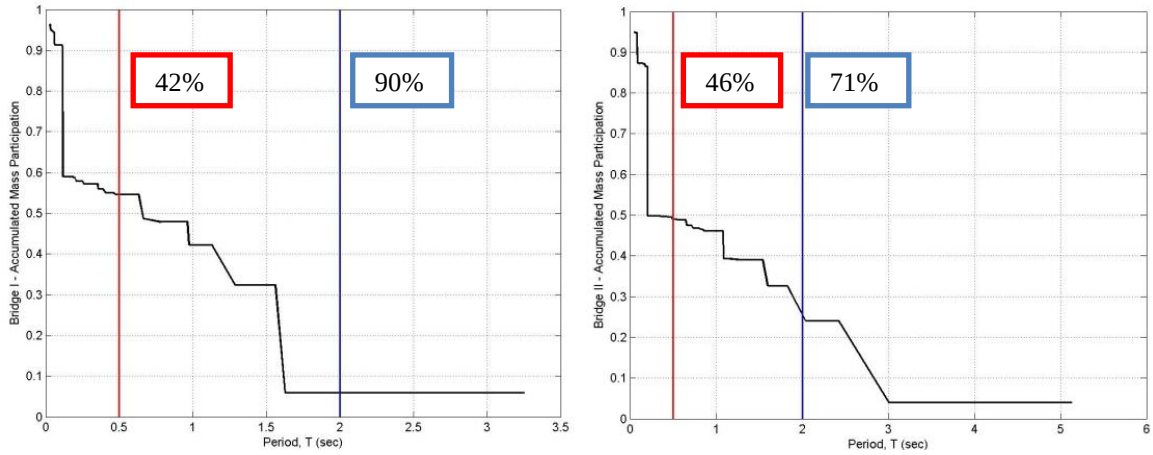

Figure 8: Accumulated mass participation ratio (vertical) vs. Period, T (sec)

The selected ground motions were scaled by utilizing the PGA scaling procedure. The peak vertical ground acceleration among all 11 records is 0.834g. All vertical ground motion records, whether pulse-like or ordinary, were scaled to this peak ground acceleration. For each record, only the horizontal component with the largest PGA was applied in the longitudinal direction of the bridge. Each horizontal ground motion component was scaled with the same scaling factor of its vertical counterpart to keep the V/H ratios constant.

Set	Event	Station	Vertical	Horizontal		Site	Dist.	V/H	scale factor	Tp^{wt}	Energy Ratio	Reference Name
			PGA [g]	PGA [g]	PGA [g]		km			[sec]		
Coherent Pulse	Northridge [1994] Mw = 6.69	Newhall - W Pico Canyon Rd.	0.290	0.455	0.325	D	5.50	0.64	2.88	3.50	0.276	NO-NHWPCRD
		Canyon Country - W Lost Cany	0.318	0.482	0.410	D	12.40	0.66	2.62	4.55	0.277	NO-CCWLC
	Chi Chi [1999] Mw = 7.62	TCU120	0.162	0.225	0.193	C	7.40	0.72	5.15	13.05	0.481	CHI-TCU120
		CHY028	0.337	0.821	0.653	C	3.10	0.41	2.47	5.97	0.296	CHI-CHY028
Incoherent Pulse	Northridge [1994] Mw = 6.69	Sylmar - Con. Sta.	0.586	0.897	0.612	C	5.40	0.65	1.42	7.45	0.138	NO-SCS
	Chi Chi [1999] Mw = 7.62	TCU088	0.222	0.522	0.508	C	18.20	0.43	3.76	13.95	0.111	CHI-TCU088
		CHY080	0.724	0.968	0.902	C	2.70	0.75	1.15	7.21	0.161	CHI-CHY080
Ordinary	Northridge [1994] Mw = 6.69	Arleta - Nordhoff Fire Sta	0.552	0.344	0.308	D	8.70	1.60	1.51		0.950	NO-ARLNFS
		Beverly Hills - 14145 Mulhol	0.327	0.516	0.416	D	17.20	0.63	2.55		0.433	NO-BH14145
		Rinaldi Receiving Sta	0.834	0.825	0.487	D	6.50	1.01	1.00		0.686	NO-RRS
	Chi Chi [1999] Mw = 7.62	TCU079	0.388	0.743	0.393	C	11.00	0.52	2.15		0.446	CHI-TCU079

Table 2: Selected records for analytical investigation

3.3 Live load analysis and response measures

Moving load analyses were carried out by utilizing the tangent stiffness obtained by non-linear analysis of dead loads. The goal of the live load analysis was to obtain possible maxi-

mum demands along the bridge girders for comparison with seismic demands. The load factors used for permanent and live loads [29] are listed in Table 3. Strength II combination considers permit live loading [30]. Furthermore, the live load factor, γ_{EQ}, in Extreme I load combination [29], which represents the possibility of partial live loads during earthquakes events was assumed to be zero in order to obtain only the seismic demands. This way, a conservative comparison between maximum live load and seismic demands is allowed. In total, 4 load combinations are considered to obtain the maximum dead/live load bending moment and rotation demand on girders, one for Strength I and three for Strength II combination considering the restricted permit loads.

Limit State	Permanent Load	LL_{HL93}	LL_{Permit}	EQ
STRENGTH I	1.25	1.75	-	-
STRENGTH II	1.25	-	1.35	-
EXTREME I	1	γ_{EQ}	-	1
SERVICE II	1	1.3	-	-

Table 3: Load combinations and load factors

The deflection criterion was checked according to the Service II limit state. The maximum vertical deflections at mid-span (center of main span) are 0.70ft and 1.30ft for Bridges I and II, respectively. For most long-span cable-stayed bridges, acceptable deflection values are in between 1/400 and 1/500 of the central span length, which equals to 2.24ft and 4.40ft (1/500) for Bridge I and Bridge II, respectively.

3.4 Dynamic analysis results

Geometrically-nonlinear time history analyses were conducted by utilizing the dead load deformed state initial stiffness conditions to obtain seismic response characteristics of the bridges when subjected to the selected ground motions. Newmark implicit integration scheme was employed with $\delta = 0.5$and $\alpha = 0.25$ values. A time step, $\Delta t = 0.02$ which allows high frequency modes to participate in response, was adopted. Here, it is important to note that usually a sensitivity analysis should be carried out to determine the time step. However, for simplicity the commonly accepted and suggested time step value was used in this study.

Two bridges were analyzed with the selected 29 ground motions which are listed in Table 2. The envelope maximum responses obtained from dead load and live load combinations are compared with the seismic demands resulting from only horizontal, H, and horizontal and vertical, H+V, ground motions. Global and local earthquake response parameters were monitored and compared.

Figures 9 and 10 compare the bending moment and rotation demands along the girder of the Bridge I with and without vertical excitation for selected representatives of pulse-like and ordinary ground motion records from the Northridge, 1994 earthquake. All representative records are from the same distances (due to scaling) and site conditions (refer Table 2). Results are presented only from end support to the center of the main span (mid-span) since multi-support excitation was not considered in analyses. As shown in legends, the responses obtained from dynamic analyses are compared with the maximum demand values obtained from the dead and live loads.

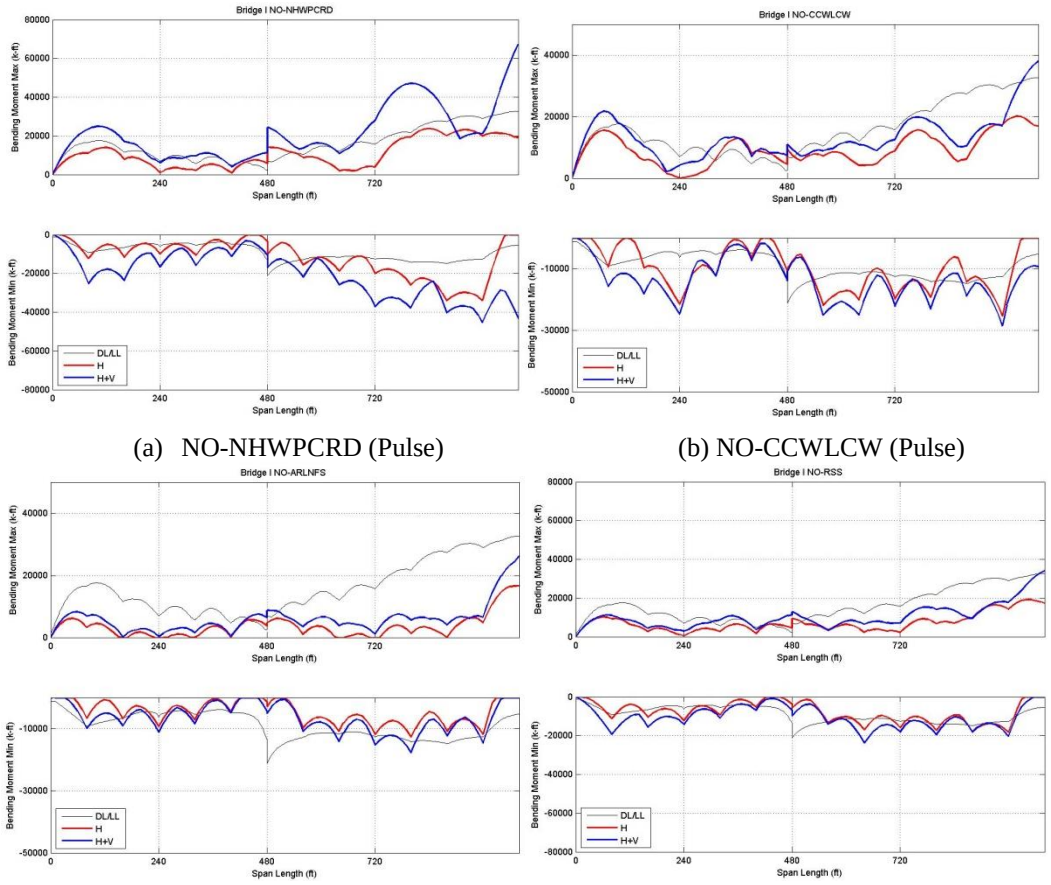

(a) NO-NHWPCRD (Pulse) (b) NO-CCWLCW (Pulse)

(c) NO-ARLNFS (Ordinary) (d) NO-RRS (Ordinary)

Figure 9: Moment demand comparison along girder (Bridge I)

From Figures 9 and 10 it can be concluded that both positive and negative moment were amplified along the bridge deck when the pulse-type vertical ground motion was included in the analysis. The moment amplification ratio at the mid-span changes from 16% to 158% for the positive bending moment and from 63% to 1137% for the negative bending moment (Figure 9 and Table 4). The reason for those exceptionally high amplification ratios, especially in negative bending moment, is that the negative bending moment under dead/live loads and horizontal ground motion is very small (Table 4).

In some cases although the record consists of strong velocity pulses, high amplification of moment demand was not observed. For example, although NO-CCWLCW (Figure 9b and 11b) record classified as "pulse-like" and has almost the same energy ratio with NO-NHWPCRD (Table 2), its response amplification is accumulated in a short period range at round 2 seconds (Figure 10) where the response amplification for NO-NHWPCRD record is on a larger period range (Figure 9a and 11a). This may result from the different response amplification characteristics due to carried total seismic energy by wave train as discussed earlier (Figure 10). Furthermore, Bridge I has a mass participation ratio of only about 10% around the 2 second period as shown in Figure 8. Thus, NO-CCWLCW ground motion record excites a smaller portion of mass when compared to NO-NHWPCRD record. Furthermore, a relationship between the pulse properties and amplification of response over the medium-to-long period range should be quantitatively defined. In addition, it is important to remember that PGA scaling was used in this study and medium-to-long period range of structures is sensitive to velocity rather than acceleration. Thus, developing a scaling procedure that takes into account

the sensitivity of different period ranges could increase the consistency between the seismic demands and allow a better comparison. Such a scaling procedure may be possible with an energy based approach. However, both developing an identification procedure of pulse characteristics, i.e. pulse period, and such an elaborate scaling procedure for ground motions are beyond the scope of this study.

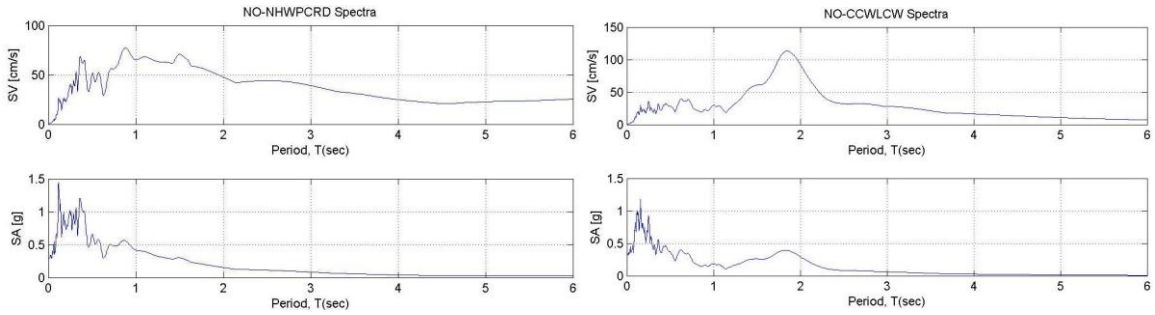

Figure 10: Response amplification comparison for NO-NHWPCRD and NO-CCWLCW

Furthermore, Figures 9 (c) and (d) show the moment demand along the bridge deck from representative ordinary vertical ground motion. It is important to note that these two records are commonly utilized ground motion records in the investigation of vertical ground motion effects. As depicted in the figures, the inclusion of the vertical component in the analysis leads to a very small amplification of moment demand when it is compared to the case of pulse presence, and usually maximum moment demands do not exceed the demand values provided by vehicular load. The moment demand comparison between all selected records for Bridge I are given in Table 4 with amplification ratios with respect to DL/LL maximum and positive and negative bending moment demand values for both H and H+V cases at mid-span.

Set	Reference Name	Maximum Positive Moment (k-ft)			Amplification Ratio (%) w.r.t DL/LL	Contribution of VGM to maximum negative moment (%)	Maximum Negative Moment (k-ft)			Amplification Ratio (%) w.r.t DL/LL
		DL/LL	HGM	H+VGM	H+VGM		DL/LL	HGM	H+VGM	H+VGM
Coherent Pulse	NO-NHWPCRD	32613.8	19275	67358	106.5	249.5	-5252	0	-43346	725.3
	NO-CCWLC		16945	38062	16.7	124.6		0	-9302	77.1
	CHI-TCU120		19423	84093	157.8	333.0		0	-64963	1136.9
	CHI-CHY028		30069	53911	65.3	79.3		-6758	-37992	623.4
Incoherent Pulse	NO-SCS		18905	42964	31.7	127.3		0	-8549	62.8
	CHI-TCU088		16177	41991	28.8	159.6		0	-11581	120.5
	CHI-CHY080		18015	37940	16.3	110.6		0	-13259	152.4
Ordinary	NO-ARLNFS	32613.8	16655	26219	-19.6	57.4	-5252	0	0	-
	NO-BH14145		18286	34179	4.8	86.9		0	-11340	115.9
	NO-RRS		17371	34037	4.4	95.9		0	0	-
	CHI-TCU079		16305	16433	-49.6	0.8		0	0	-

Table 4: Bridge I - Summary of analysis results

From Figure 11(c) and (d), it can be concluded that the amplification of rotation demands along the deck due to ordinary vertical ground motions are relatively smaller when compared to the pulse-like counterparts. Similarly, increase in both positive and negative bending moment rotations are also observed along the Bridge II deck. However, the assessment of the increase in rotation demands needs special attention and requires a more detailed modeling approach, i.e. support conditions. Thus, this study focuses only on the moment demand amplification in detail.

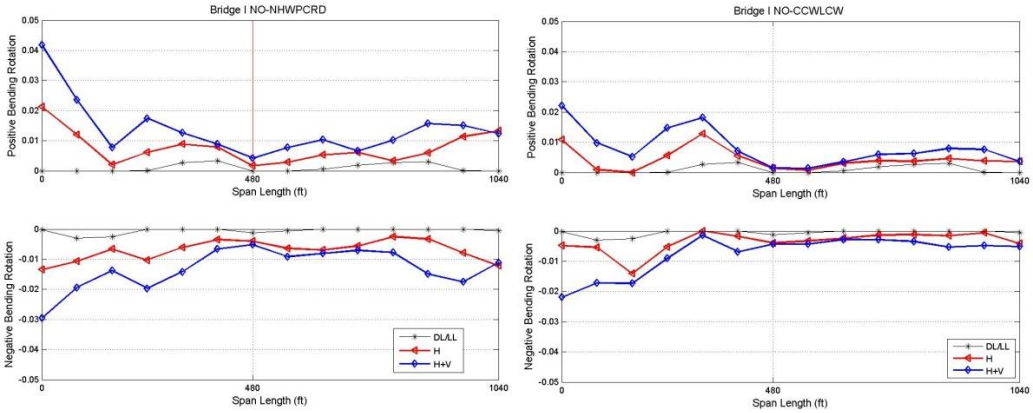

(a) NO-NHWPCRD (Pulse) (b)NO-CCWLCW (Pulse)

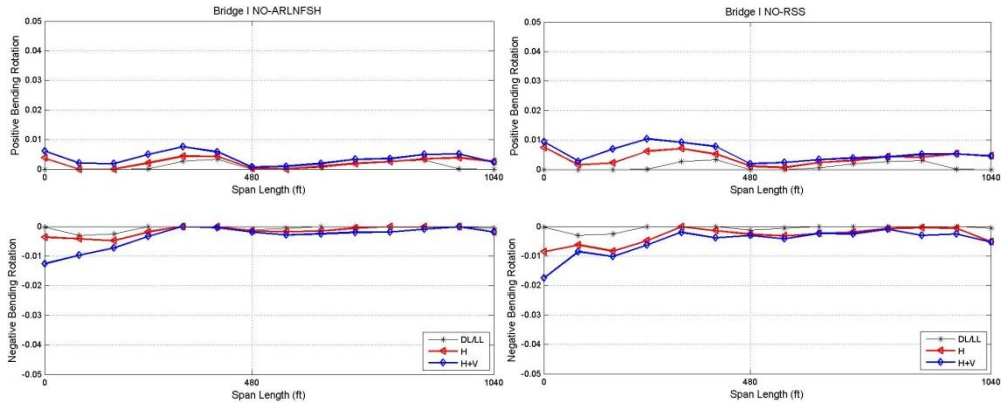

(c) NO-ARLNFS (Ordinary) (d) NO-RRS (Ordinary)

Figure 11: Rotation demand comparison along girder (Bridge I)

Table 5 provides comparison between the moment amplification ratios at mid-span obtained from all selected records with respect to DL/LL maximum for Bridge II. The table shows that the contribution to negative and positive bending moment, especially at the mid-span of the bridge deck, by coherent type pulse-like vertical ground motion is significantly more than ordinary vertical ground motion. The moment amplification ratio at the mid-span changes from 20% to 355% for the positive bending moment and from 0% to 2133% for the negative bending moment. The reason for those exceptionally high amplification ratios, especially in negative bending moment, is that the negative bending moment under dead/live loads and horizontal ground motion is very small.

Set	Reference Name	Maximum Positive Moment (k-ft)			Amplification Ratio (%) w.r.t DL/LL	Contribution of VGM to maximum negative moment (%)	Maximum Negative Moment (k-ft)			Amplification Ratio (%) w.r.t DL/LL
		DL/LL	HGM	H+VGM	H+VGM		DL/LL	HGM	H+VGM	H+VGM
Coherent Pulse	NO-NHWPCRD	74561.9	76724.95	168631.75	126.2	119.8	-15973.5	-8823.831	-45177.85	182.8
	NO-CCWLC		47596.122	143967.89	93.1	202.5		0	-80095.88	401.4
	CHI-TCU120		83225.718	339355.81	355.1	307.8		-21516.91	-356648.5	2132.8
	CHI-CHY028		65165.693	143150.08	92.0	119.7		-2859.393	-94046.65	488.8
Incoherent Pulse	NO-SCS		73467.654	89610.582	20.2	22.0		0	-42893.12	168.5
	CHI-TCU088		43724.151	89606.636	20.2	104.9		0	-5824.326	-
	CHI-CHY080		58385.957	96427.725	29.3	65.2		0	-29571.29	85.1
Ordinary	NO-ARLNFS		44188.922	111381	49.4	152.1		0	-30814	92.9
	NO-BH14145		66248.228	87633.841	17.5	32.3		-1117.707	0	-
	NO-RRS		53536.973	84410.399	13.2	57.7		0	-1565.612	-
	CHI-TCU079		56747.378	77758.79	4.3	37.0		0	-3486.802	-

Table 5: Bridge II - Summary of analysis results

When Table 4 and 5 are compared, the contributions to seismic moment demands at the mid-span vary in some cases of ground motion records for Bridge I and II as expected. For example, when NO-CCWLCW record is considered the negative bending moment amplification ratios are 77.1% and 401.4% for Bridge I and Bridge II, respectively. However, when NO-NHWPCRD record is considered, the moment amplification ratios are 725.3% and 182.8% for Bridge I and Bridge II, respectively. Thus, NO-CCWLCW record results in higher amplification ratio for Bridge I than NO-NHWPCRD record. On the contrary, NO-CCWLCW record results in a smaller amplification ratio for Bridge II than NO-NHWPCRD record. Here it is important to note that both records are classified as "pulse-like" and have almost the same energy ratio (Table 2). The change in response amplification trends of the two ground motions is due to different dynamic behavior characteristics of the two bridges as pointed out earlier. The mass distribution over the periods, the characteristics of the ground motion, and response amplification characteristics of the pulse are the parameters that cause different seismic response characteristics. The largest amplification factors are obtained from the Chi-Chi earthquake records for both bridges. This is mainly due to the large magnitude of this event. The larger the magnitude, the more coherent the pulse is. Furthermore, the input of seismic energy carried by the pulse is also increasing as the magnitude of the event increases. Thus, the response amplification is more coherent in a larger period range for large magnitude earthquake events when compared to the records from smaller magnitude earthquakes.

4 CONCLUSIONS

In this paper, strong velocity pulse features in vertical ground motion records and their effects on a class of cable-stayed bridge structures are investigated. The most important findings are summarized below.

The existence of a vertical strong velocity pulse tends to reduce the high frequency content of the record and hence increase the seismic demand on medium-to-long period structures. For the structures considered and the earthquake record set used, the bending moment and rotation demands along the bridge deck are substantially increased with respect to maximum dead and live load demands due to pulse-like vertical ground motion records. Since the assessment of rotation demands requires a more detailed modeling approach, i.e. support conditions, the results of this study focuses on the assessment of bending moment demands. The high increase in moment was observed at the center of the main span (mid-span) for both bridges. The increase in positive moment at the mid-span is between 16% and 158% for Bridge I and between 20% and 355% for Bridge II. The corresponding negative bending moment increase is between 63% and 1137% for Bridge I and between 0% and 2133% for Bridge II. The reason for such exceptionally high amplification ratios, especially in negative bending moment, is that the negative bending moment under dead and live loads and horizontal ground motion is very small. It was also observed that the response amplification characteristics of the pulse-like vertical ground motion records related to the pulse characteristics such as the coherency of the pulse signal and the pulse period. The characteristics of the velocity pulse are closely related to the source parameters, i.e. geometry and dimension of the fault, slip duration, correlation between directivity and fling step, and size of asperities. For instance, the most distinct observation is that the coherency of the pulse signals increases as the magnitude of the event increases which often results in longer pulse periods. Further investigation of the pulse characteristics and their correlations with the above-mentioned parameters is required to gain better understanding of the response amplification features of the pulse-like vertical ground motions.

The results also suggest that observations from only the acceleration or velocity spectrum may be misleading in assessing the damage potential of pulse-like vertical ground motion rec-

ords and hence they need to be examined concurrently. In a similar manner, utilizing only one ground motion parameter, e.g., peak ground acceleration, to scale the ground motions could result in unreliable assessment of seismic demand when pulse-like vertical ground motion is considered. Especially in the case of structures which have complex and coupled modes of vibration, i.e. cable-stayed bridges, a scaling procedure that is sensitive to all vibration periods would provide more realistic seismic demand assessment. Such a scaling procedure may be based on an energy criterion and provide better insight into the differences of the response amplification characteristics between normal and pulse-like vertical ground motions.

Taking into account the above observations, medium-to-long period bridge decks subjected to pulse-like vertical components of earthquake strong-motion could be more vulnerable than those subjected to the horizontal ground motion only or combined horizontal and ordinary vertical ground motions. Therefore, incorporating a vertical pulse model for the development of near-fault ground motions and including pulse-like vertical ground motion in the analysis is recommended for reliable seismic assessment and design of medium-to-long period structures in the vicinity of active faults.

REFERENCES

[1] Golesorkhi, R., and Gouchon, J. (2002). "Near-source effects and correlation to recent recorded data", Proceedings, 6th U.S. National Conference on Earthquake Engineering, Seattle, Wash.

[2] Hall, J. F., Heaton, T. H., Halling, M. W., and Wald, D. J. (1995). "Near source ground motion and its effects on flexible buildings", Earthquake Spectra, Vol. 11(4), 569–605.

[3] Heaton, T.H., Hall, J.F., Wald, D.J. and Halling, M.W (1995). "Response of High Rise and Base-Isolated Buildings to a hypothetical Mw 7.0 Blind Thrust Earthquake", Science, Vol. 267, 206-211.

[4] Anderson, J. C., and V. V. Bertero (1987). "Uncertainties in establishing design earthquakes", J. Struct. Eng. 113, no. 8, 1709–1724.

[5] Alavi, B., and Krawinkler H. (2001). "Effects of near-fault ground motions on frame structures", Blume Center Report 138, Stanford, California.

[6] Manfredi, G., Polese, M., and Cozenza, E. (2000). "Cyclic demand in the near-fault area", Proceedings, 6th U.S. National Conference on Earthquake Engineering, Seattle, Wash.

[7] Kalkan E. and Kunnath S.K. (2006). "Effects of Fling-Step and Forward Directivity on the Seismic Response of Buildings", Earthquake Spectra. 22, No. 2, 367-390.

[8] Veletzos, M. J., Restrepo, J. I., Seible, F., 2006 : Response of precast segmental bridge superstructures, Report submitted to Caltrans - SSRP-06/18, University of California, San Diego, California.

[9] Kim, S. J. and Elnashai, A. S. (2008). "Seismic Assessment of RC Structures Considering Vertical Ground Motion", Report No. MAE 08-03, University of Illinois at Urbana-Champaign, Urbana, Illinois.

[10] Kunnath, S. K., et al. (2008). "Development of guidelines for incorporation of vertical ground motion effects in seismic design of highway bridges", Report No. CA/UCD-SESM-08-01, University of California, San Diego, California

[11] Somerville, P.G., et al. (1997). "Modification of empirical strong ground motion attenuation relations to include the amplitude and duration effects of rupture directivity", Seismological Research Letters, Vol. 68(1), 199-222.

[12] Somerville, P.G. (2002). "Characterizing near fault ground motion for the design and evaluation of bridges" Proceedings of the Third National Seismic Conference and Workshop on Bridges and Highways. *This paper is posted on the test bed website.*

[13] Allen, C. R., Brune, J. N., Cluff, L. S., and Barrows, A. G. Jr. (1998). "Evidence for Unusually Strong Near-fault Ground Motion on the Hanging Wall of the San Fernando Fault During the 1971 Earthquake", Seismological Research Letters, Vol. 69(6), 524-531.

[14] Brune, J. N. (1996). "Particle Motions in a Physical Model of Shallow Angle Thrust Faulting", Earth and Planetary Sciences, Proceedings of the Indian Academy of Sciences, Vol. 105 (2), L197-L206.

[15] Shi, B., Anooshehpoor, A., Brune, J. N., and Zeng, Y. (1998). "Dynamics of Thrust Faulting: 2D Lattice Model, Bulletin of the Seismological Society of America, Vol. 88, 1484–1494.

[16] Shi, B., Brune, J. N. (2005). "Characteristics of Near-Fault Ground Motions by Dynamic Thrust Faulting: Two-Dimensional Lattice Particle Approaches", Bulletin of the Seismological Society of America, Vol. 95, 2525–2533.

[17] Oglesby, D. D., and Day, S. M. (2001). "Fault Geometry and the Dynamics of the 1999 Chi-Chi (Taiwan) Earthquake", Bulletin of the Seismological Society of America, Vol. 91(5), 1099-1111.

[18] Oglesby, D. D., and Day, S. M. (2001). "The effect of the Fault Geometry on the 1999 Chi-Chi (Taiwan) Earthquake", Geophysical Research Letters, Vol. 28, 1831-1834.

[19] Oglesby, D. D., Archuleta, R. J. and Nielsen, S. B. (1998). "Earthquakes on Dipping Faults: The Effect of Broken Symmetry", Science, Vol. 280, 1055-1059.

[20] Oglesby, D. D., Archuleta, R. J. and Nielsen, S. B. (2000). "The Three-Dimensional Dynamics of Dipping Faults", Bulletin of the Seismological Society of America, Vol. 90(3), 616-628.

[21] Rowshandel, B. (2006). "Incorporating Source Rupture Characteristics into Ground-Motion Hazard Analysis Models", Seismological Research Letters, Vol. 77(6), 708-722.

[22] Mena, B., Mai, P. M. (2010). "Selection and Quantification of Near-Fault Velocity Pulses Due to Source Directivity", ETH Zurich – Report

[23] Kawase, H. and Aki, K. (1990). "Topography effect at the critical SV-wave incidence: Possible explanation of damage pattern by the Whittier Narrows, California, earthquake of 1 October 1987", Bulletin of the Seismological Society of America, Vol. 80, 1-30.

[24] Silva, W. (1997). "Characteristics of vertical strong ground motions for applications to engineering design," FHWA/NCEER Workshop on the National Representation of Seismic Ground Motion for New and Existing Highway Facilities; Burlingame; CA;

Proceedings, Technical Report NCEER-97-0010, National Center for Earthquake Engineering Research, Buffalo, New York.

[25] Baker, J. W. (2007). "Quantitative Classification of Near-Fault Ground Motions Using Wavelet Analysis", Vol. 97(5), 1486-1501.

[26] Bray, J. D., and Rodriguez-Marek, A. (2004). "Characterization of forward-directivity ground motions in the near-fault region." Soil Dynamics and Earthquake Engineering, 24, 815-828.

[27] Nazmy, A. S., and Abdel-Ghaffar, A. M. (1987). "Seismic Response Analysis of Cable-Stayed Bridges Subjected to Uniform and Multi-Support Excitations." Report No. 87-SM-1, Department of Civil Engineering, Princeton University, Princeton, N.J.

[28] Abdel-Ghaffar, A. M. and Nazmy, A. S. (1991). "3-D nonlinear seismic behavior of cable-stayed bridges." Journal of Structural Engineering, ASCE, 117 (11), pp. 3456-3476.

[29] AASHTO (2011). LRFD Bridge Design Specifications - 4th edition. American Association of State Highway and Transportation Officials, Washington, D. C.

[30] Caltrans (2011). "California Amendments to the AASHTO LRFD Bridge Design Specifications –Fourth Edition".